Articles

Application of a Perrin-like Kinetics Model to the Photochemical Degradation of Polymers

Bevin C. Daglen and David R. Tyler*

Department of Chemistry, University of Oregon, Eugene, Oregon 97403

Received July 31, 2008; Revised Manuscript Received October 28, 2008

ABSTRACT: The photochemical degradation rates of two solid-state polymer systems, a cross-linked poly(vinyl chloride) and a segmented polyurethane, that contain metal−metal bonds in the backbone were found to exhibit biphasic behavior. The polymers initially degraded quickly but then degraded slower at longer irradiation times. To investigate the origin of this biphasic rate phenomenon, the data were fit to four kinetic models: first- and second-order rate equations, a simple-diffusion model, and a diffusion-controlled model. None of the models adequately described the data. A new kinetic model was developed to describe a biphasic photodegradation rate that was inspired by Perrin's model of fluorescence decay rates. Using this new Perrin-like model, the derived rate equation fit the data very accurately. The resulting fitting parameters obtained as a function of reaction temperature were also consistent with the model. To investigate the versatility of this Perrin-like model, literature data for the irradiation of polyoxymethylene were also evaluated. It was found that this system also exhibited Perrin-like kinetics.

Introduction

Photochemically degradable polymers are used in a number of applications, including photolithography, degradable consumer plastics, and in the farming technique known as plasticulture.[1−11] Because of their widespread use, considerable research is devoted to developing new photochemically degradable polymers with improved performance. A major goal is to devise photodegradable polymers with a tunable onset of degradation and with a specific degradation rate. In order to design a polymer with such properties, it is necessary to identify the experimental parameters that affect degradation rates and to determine how those parameters affect the degradation mechanism. A typical first step in these studies is to determine the kinetics of the degradation reaction. An interesting observation from these kinetic studies is that the photodegradation rates of solid-state polymers are often biphasic, showing a relatively fast rate during the initial period of irradiation but a slower rate at longer times (Figure 1).[12,13] Several hypotheses have been proposed to explain this observation, but no definitive explanation has come forth. As part of our ongoing study of polymer photodegradation, we began an investigation into the origin of the biphasic behavior.

Several challenging experimental problems hinder the rigorous experimental mechanistic exploration of polymer photodegradation. One of the difficulties is that polymer degradation is mechanistically complicated. This is not to say that the mechanisms are not understood; in fact, they are understood in detail.[14−17] Rather, the mechanisms are intricate, often involving multiple steps, cross-linking, and side reactions; this makes pinpointing the effects of various experimental parameters difficult. To circumvent these mechanistic complexities and therefore make it less difficult to interpret data and obtain fundamental insights, we use three key experimental strategies in our investigations. First, we study problems using special photodegradable polymers of our own design that contain metal−metal bonds along the backbone.[18−21] These polymers are photodegradable because the metal−metal bonds can be cleaved with visible light and the resulting metal radicals captured with an appropriate radical trap, typically a carbon−halogen bond or O_2 (Scheme 1).[22,23] By studying these polymers, we are able to extract information without the mechanistic complications inherent in the degradation mechanisms of organic radicals. (For example, metal radicals do not lead to cross-linking, so we can avoid this complicating feature found with organic radicals.)

The second key experimental strategy is to use polymers that have built-in radical traps, namely C−Cl bonds (Scheme 2).[24,25] By eliminating the need for external oxygen to act as a trap, the complicating kinetic features of rate-limiting oxygen diffusion can be excluded. The third experimental strategy is to use the distinctive M−M bond chromophore to monitor the photodegradation reactions by electronic absorption spectros-

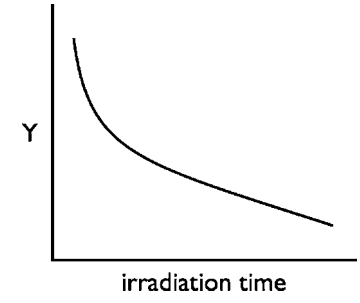

Figure 1. Plot illustrating the typical biphasic decay for the photodegradation of a polymer. The data represented on the *y*-axis will vary with the degradation monitoring technique; two examples are radical concentration in the case of ESR experiments or number-average molecular weight obtained from gel permeation chromatography.

* Corresponding author. E-mail: dtyler@uoregon.edu.

10.1021/ma8017487 CCC: $40.75
Published on Web 11/26/2008

Scheme 1. Photochemical Reaction of a Polymer with Metal−Metal Bonds along Its Backbone

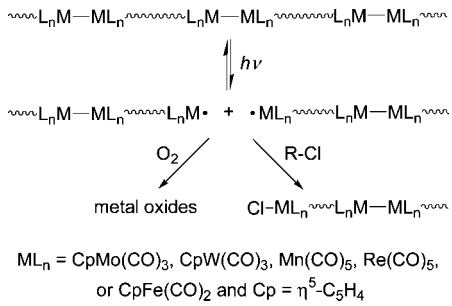

ML_n = $CpMo(CO)_3$, $CpW(CO)_3$, $Mn(CO)_5$, $Re(CO)_5$, or $CpFe(CO)_2$ and Cp = η^5-C_5H_4

copy. The use of UV−vis methods to quantify and compare the various degradation rates is a time-saving technique because polymer degradation reactions have typically been monitored by stress testing, molecular weight measurements, or attenuated total reflection (ATR) spectroscopy, all of which can be laborious and time-consuming.

In this paper we present a new explanation for the biphasic photochemical degradation rates of polymers. Specifically, a mechanistically based four-parameter equation is presented and tested. The new model was assessed on two polymers that contain M−M bonds in their backbones: one a cross-linked poly(vinyl chloride) and the other a polyurethane with soft and hard segments. To investigate the range of application of this new model, literature data for the photodegradation of a polyoxymethylene were also tested.[26] The coefficients extracted from the fits were evaluated as a function of reaction temperature, which led to further mechanistic insights.

Materials and Methods

Materials. All manipulations were carried out using standard Schlenk techniques or in a Vacuum Atmospheres Co. glovebox under a nitrogen atmosphere. Unless otherwise noted, HPLC grade solvents were deoxygenated by passage through columns of alumina and copper oxide under an argon atmosphere. (η^5-$C_5H_4CH_2$-$CH_2OH)_2Mo_2(CO)_6$ was prepared as previously described.[20,27] Carboxylated poly(vinyl chloride) (1.8 wt %) was purchased from Aldrich. Thionyl chloride (Fluka, 99%) was stored in a desiccator. 1-(Chloromethyl)-2,4-diisocyanatobenzene (97%) was obtained from Aldrich, stored in the drybox, and used as received. 1,4-Butanediol (98%, Aldrich) was distilled under reduced pressure and stored under nitrogen in the drybox. Tolylene 2,4-diisocyanate-terminated poly(propylene glycol) (3.6 wt % isocyanate; $M_n \sim$ 2300) was obtained from Aldrich. Dibutyltin diacetate (DBTA, Aldrich) was stored in the refrigerator in the dark.

Instrumentation. Infrared spectra were recorded on a Nicolet Magna 550 FT-IR spectrometer with OMNIC software. Thermal transitions were determined using a dynamic mechanical analyzer Q800 by TA Instruments. The modulus measurements were carried out at room temperature using an Instron 4444 mechanical tester and are reported as stress (MPa)/% strain.

Synthesis of the Polymers. PVC−COCl, polymer **1**, and polymer **2** were synthesized as previously described.[28]

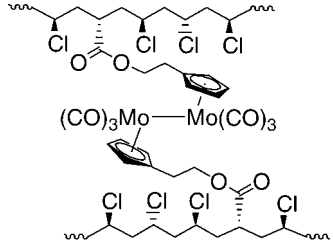

1

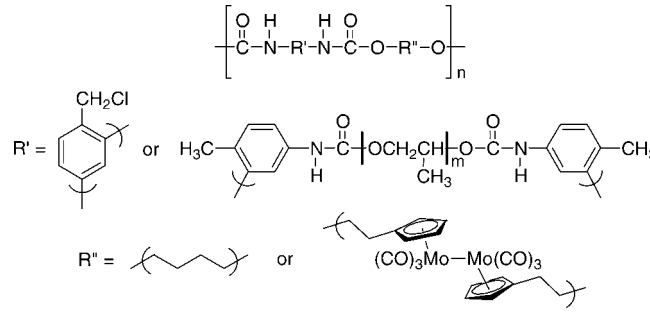

2

Irradiation Techniques. All samples were prepared in a drybox under red light, transferred to a temperature-controlling unit, and allowed to thermally equilibrate for an hour. The dimensions of the solid polymer films were on average 0.08 mm × 5.0 mm × 20 mm. The samples were irradiated using a Nd:YAG laser tuned to 532 nm. The transmittance value was collected every 3 s for 50 min using an Oriel Merlin radiometry system.[29] The molybdenum dimer concentration values were calculated using Beer's law (ε = 1995 M^{-1} cm^{-1} at 532 nm) and normalized by dividing by the starting concentration. Degradation data were collected several times on each polymer sample to ensure reproducibility of the data.

Literature Data Capture. The original data were "captured" using pixel conversion.[30] The data image was scanned from the original journal article and opened in previewing software. The cursor was used to locate the pixel coordinates for the data points in the graph as well as the origin and maxima of the *x*- and *y*-axes. The pixel values for the data were recorded in an array and converted to the "original" values, *X* and *Y*, using the following previously derived eqs 1 and 2:[30]

$$X = X_{\min} + (pX - pX_{\min})\frac{X_{\max} - X_{\min}}{pX_{\max} - pX_{\min}} \quad (1)$$

$$Y = Y_{\min} + (pY_{\min} - pY)\frac{Y_{\max} - Y_{\min}}{pY_{\min} - pY_{\max}} \quad (2)$$

where X_{min}, Y_{min}, X_{max}, and Y_{max} are the axes origin and extreme values extracted from the plot, pX_{min}, pY_{min}, pX_{max}, and pY_{max} are the corresponding pixel coordinates for the axes, and pX and pY are the pixel coordinates for the data points of interest. The generated arrays of "original" data were fit to model equations using IGOR Pro Carbon.

Results and Discussion

Polymer Preparation. Polymers **1** and **2** were synthesized as previously described.[28,31] In brief, polymer **1** was synthesized by cross-linking a poly(vinyl chloride) prepolymer (functionalized with 2.1 wt % carboxyl content) with (η^5-$C_5H_4CH_2$-$CH_2OH)_2Mo_2(CO)_6$. Polymer **2** was synthesized by reacting a poly(propylene glycol) prepolymer and 1-(chloromethyl)-2,4-diisocyanatobenzene with 1,4-butanediol and (η^5-$C_5H_4CH_2$-$CH_2OH)_2Mo_2(CO)_6$. These syntheses afforded polymers that contain a photosensitive chromophore, $-CH_2C_5H_4(CO)_3Mo-Mo(CO)_3C_5H_4CH_2-$, that homolyzes when exposed to visible light (λ_{max} = 390 nm for the $\sigma \rightarrow \sigma^*$ transition and 510 nm for the $d\pi \rightarrow \sigma^*$ transition).[32,33] The polymer films were solution cast in a Teflon mold, forming films red in color with thicknesses ranging from 0.05 to 0.10 mm. This range of thickness was optimal for absorbing 90−99% of the photons used for irradiation in the photodegradation studies. Previous work showed that the photogenerated metal radicals ($-CH_2C_5H_4(CO)_3Mo^{\bullet}$) could be trapped in the solid state by the radical trapping unit C−Cl, resulting in the formation of metal−halide bonds ($-CH_2C_5H_4(CO)_3Mo-Cl$) and net degradation of the polymer.[31] The semicrystalline nature of polymers **1** and **2** was

Scheme 2. Example of a Photochemical Reaction of a Polymer with a Built-In Radical Trap[a]

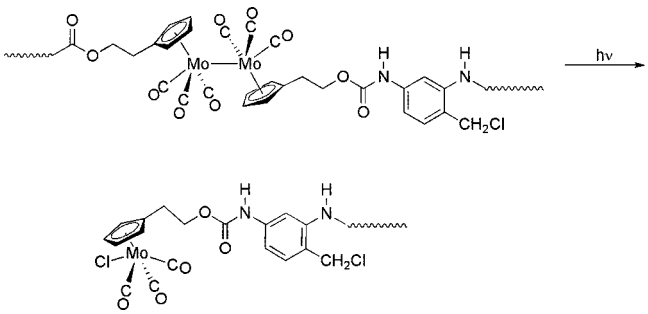

[a] The source of the Cl atom that captures the Mo radical is the C−Cl bond contained in the polymer.

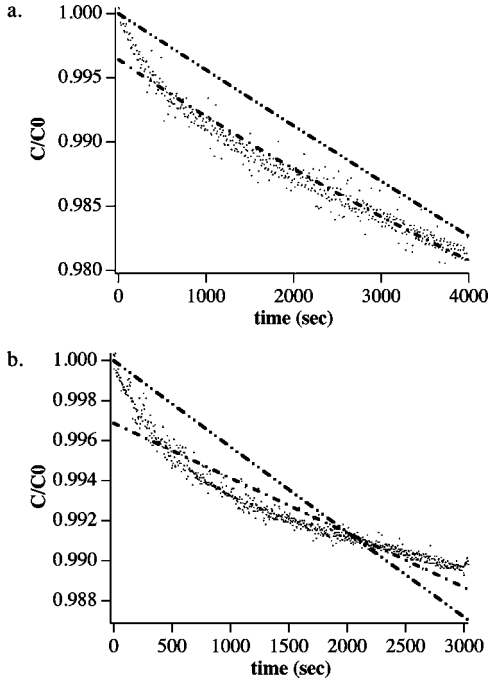

Figure 2. Relative $-CH_2C_5H_4(CO)_3Mo-Mo(CO)_3C_5H_4CH_2-$ concentration as a function of irradiation time at room temperature for polymer **1** (a) and **2** (b) with fits for the first-order (-•-) and second-order (-••-) equations.

evaluated using infrared spectroscopy. For polymer **1**, the presence of both crystalline and amorphous regions was confirmed by observing IR absorption bands at 1425 and 1436 cm^{-1}, which correspond to the CH_2 bending modes in crystalline and amorphous regions, respectively.[34,35] For polymer **2**, the presence of both crystalline and amorphous regions was confirmed by observing IR absorption bands at 1737, 1712, and 1700 cm^{-1}, which correspond to the urethane C=O stretching frequencies of the non-hydrogen-bonded, loosely hydrogen-bonded, and strongly hydrogen-bonded modes, respectively.[36−40] The glass transition temperatures for polymers **1** ($T_g = 65 \pm 4$ °C) and **2** ($T_g = 55 \pm 3$ °C) were determined by dynamic mechanical analysis.

Fitting the Biphasic Photodegradation Data. Concentration data for the photodegradation of polymers **1** and **2** as a function of irradiation time are shown in Figure 2. (Note the data in Figure 2 were normalized by dividing the concentration values by the initial concentration.) The traces in Figure 2 exhibit biphasic character, showing a relatively fast rate during the initial period of irradiation but a slower rate at longer times. In an attempt to fit the data, several mechanistic models were evaluated. Owing to the fact that the plots are not linear, the reactions are not the usual simple zeroth-order photochemical reactions. (Note, however, that the slopes at long reaction times do appear linear.) To test for the potential origin of the biphasic kinetics, the data were fit to the expression $C/C_0 = Ae^{-kt}$, which represents first-order kinetics in the disappearance of starting material. In this case, the reaction kinetics would be dependent on the concentration of the molybdenum dimer chromophore. The first-order fits to the degradation data for polymers **1** and **2** are shown in parts a and b of Figure 2, respectively. The fits clearly do not represent what is occurring at short reaction times. The second-order equation, $C/C_0 = (1 + Bt)^{-1}$, was also evaluated, but the fits were no better (Figure 2a,b).

It was hypothesized that the biphasic behavior exhibited by these polymers may be attributed to unique reactivity in the solid state. One possible explanation is that the reaction rate is not solely determined by a specific chemical transformation but rather by diffusion processes. One representation of diffusion behavior, as observed for the disappearance of starting material, is the simple-diffusion equation, $C/C_0 = (1 + Dt^{1/2})^{-1}$.[41] Simple-diffusion kinetics were used to describe the degradation of solid-state polyolefins where the decay of the photogenerated radicals was hypothesized to be controlled either by oxygen diffusion into the polymer material or by radical migration to the crystalline surfaces where radical-trapping oxygen was present.[42] The fits of the degradation data for polymers **1** and **2** to the simple-diffusion equation are shown in Figure 3a,c. Note that, although the simple-diffusion model is a more promising fit than a simple first- or second-order equation, it clearly overestimates the reaction rates at both short (see Figure 3b,d) and long reaction times and is consequently not a suitable description of this system.

Waite developed a modification of the simple-diffusion model called the diffusion-controlled model.[43−45] This model describes bimolecular reactions in the solid state or in highly viscous solutions where both diffusion and spatial distribution of the reactive species are taken into account. The model (described by the equation $C/C_0 = (1 + Bt + Dt^{1/2})^{-1}$) has been used to fit the radical decay kinetics of several photodegradation reactions of polyolefins and polyethers as monitored by electron spin resonance spectroscopy.[26,41,46,47] Figure 3a,c shows the fits for the diffusion-controlled model developed by Waite. Like the simple-diffusion model, it can be seen (particularly in Figure 3b,d) that the diffusion-controlled model overestimates the initial reaction rate. However, in contrast to the simple-diffusion model, Waite's model does more closely represent the data at longer reaction times. Be that as it may, none of these conventionally used models could adequately describe the kinetic behavior of polymers **1** and **2**; accordingly, a new model based on Perrin kinetics was developed to explain the biphasic behavior.

Derivation of a Perrin-like Photochemical Model. There are many instances in the literature where a chemical species is converted to a single product in the same reaction vessel by two or more mechanistically different routes that possess different observed rates. One example is heterogeneous catalysis, where a reactant may experience different catalytic sites on the reactive surface.[48,49] Another example, which is the focus of this paper, involves a photoreactive species embedded in a solid polymer matrix. In particular, one consequence of the micro-heterogeneity of polymers (in polymers possessing both crystalline and amorphous regions[50]) is that a reactive species in a polymer matrix can reside in different molecular landscapes. For example, it is well-known that oxidation reactions in highly crystalline polymers have different reaction rates at the crystal grain boundaries than within the crystalline regions.[51] These two different environments result in an observed reaction rate that is a composite of two intrinsically different reaction

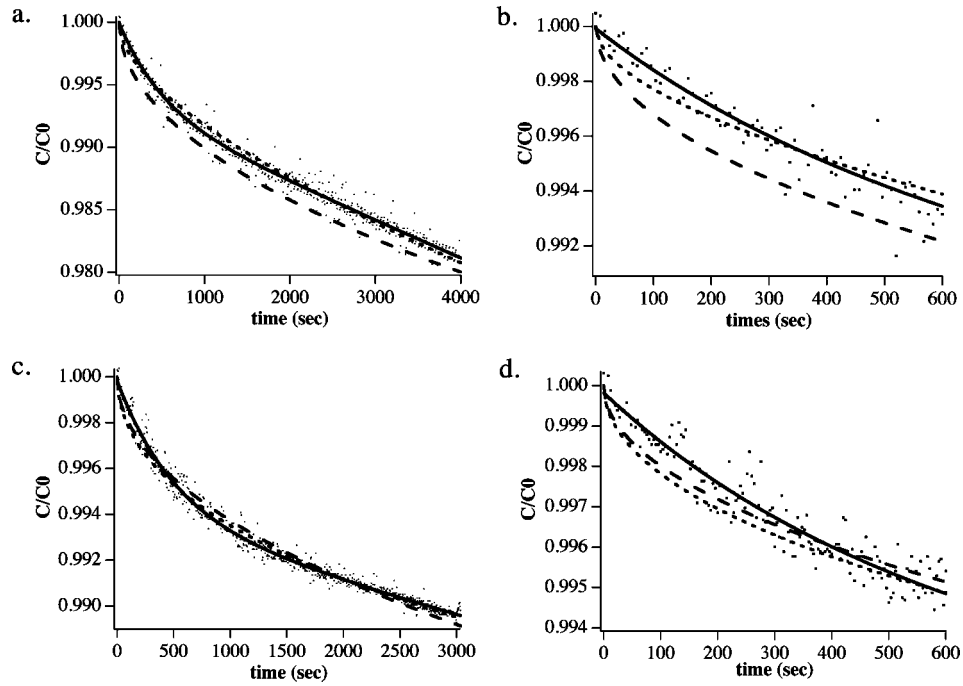

Figure 3. Relative $-CH_2C_5H_4(CO)_3Mo-Mo(CO)_3C_5H_4CH_2-$ concentration as a function of irradiation time at room temperature for polymer **1** (a, b) and **2** (c, d) with fits for the simple diffusion (— — —), diffusion-controlled (**- - -**), and Perrin-like (—) equations. The plots in (b) and (d) show the initial data in plots (a) and (c), respectively, on expanded axes.

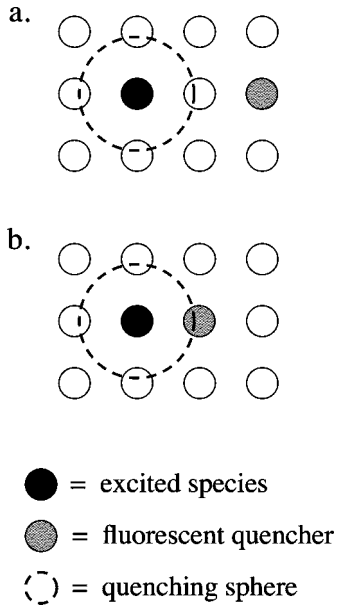

Figure 4. Perrin model used to describe the observed rates for the fluorescence decay of a chromophore in the solid state.

pathways that result in the same product. The rate equation for such a reaction can be derived from the model A → B, where reactant A consists of two components, X and Y, as expressed in eq 3.

$$[A] = [X] + [Y] \tag{3}$$

Another case found in the literature where the observed reaction rate is the combination of two separate rates was described by Perrin in the early part of the twentieth century.[52] The Perrin model, shown in Figure 4, was established to explain the observed nonexponential fluorescence decay of small molecules in solid polymers.[52,53] Perrin considered the microheterogeneity of solid-state polymers and the relative immobility of atoms in the solid state. For fluorescence decay, he proposed that when an acceptor was in the quenching sphere of an electronically excited donor molecule, the fluorescence would be quenched. Therefore, the observed rate of fluorescence decay was the combination of the decay rate of excited molecules in the presence of a quencher and the natural decay rate of molecules in the absence of a quencher. A mechanistic analogy can be made for photogenerated radical species in solid-state polymers: the observed rate of radical decay will be the combination of the rate where a radical trapping agent is in the reactive sphere of the radical and where it is not. (The term "reactive sphere" is equivalent to the term "quenching sphere" used in the case of the original Perrin model.) This is represented pictorially in Scheme 3a,b.

To generate the observed rate equations for the disappearance of the starting material as illustrated in Scheme 3, one must consider the kinetics of the photoreaction and how the coinciding individual cases affect the kinetics. For the simple case where a photon causes a singular photoreaction, the rate equation for the conversion of A to B can be written as

$$-\frac{dA}{dt} = \phi I_m(1 - 10^{-\varepsilon c_A l})\frac{S}{V} \tag{4}$$

where ϕ is the quantum yield of the reaction, I_m is the number of einsteins absorbed per unit volume and unit time, ε is the molar absorptivity, c_A is the concentration of the chromophore, l is the path length, S is the surface area, and V is the volume of the irradiated sample.[54] Equation 4 can be simplified by considering the magnitude of photon absorption by the sample. For instance, if the absorbance value is large ($\varepsilon c_A l > 2$), then $1 - 10^{-\varepsilon c_A l} \sim 1$, and the rate can be written as

$$-\frac{dA}{dt} = \phi I_m \frac{S}{V} \tag{5}$$

which is a zeroth-order reaction. Conversely, if the absorbance of the substance is small ($\varepsilon c_A l < 0.1$), then $1 - 10^{-\varepsilon c_A l} \sim 1$, and the rate can be written as

Scheme 3. Illustration of the Reaction of Photogenerated Metal Radicals with Trapping Atoms in a Solid-State Matrix[a]

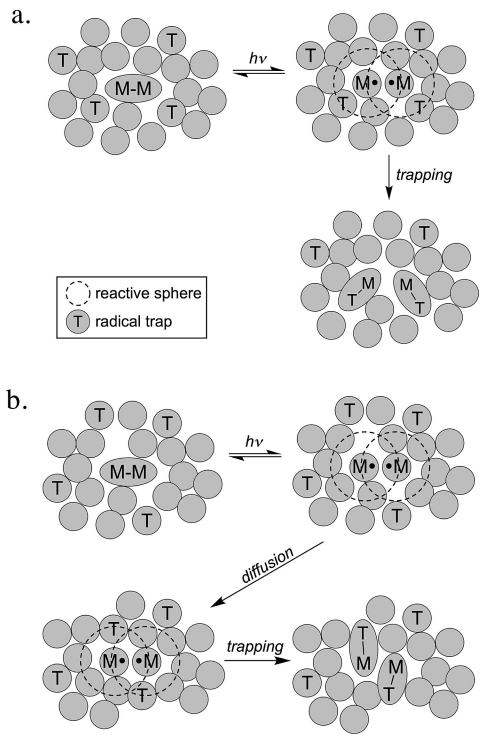

[a] In case (a), there is a trap in the reactive sphere of the metal radical. In case (b), the trap is initially outside of the reactive sphere.

$$-\frac{dA}{dt} = 2.303\varepsilon c_A l\phi I_m \frac{S}{V} = \text{constant}\cdot c_A \quad (6)$$

which is a first-order reaction. To determine the rate equation that corresponds to the individual cases illustrated in Scheme 3, the relative absorbances of each will be evaluated. An assumption is made that the experimental path lengths and molar absorptivity of both cases are the same because both species exist in the same sample and, in both cases, the absorbing species is the same. Therefore, the relative absorbances will be determined by the relative concentrations of both species. Returning to Figure 3, it is observed that <1% of the absorbing species is consumed in the initial fast reaction rate. This species, termed Y, is in very low concentration and therefore is predicted to exhibit first-order kinetics,[54] eq 7, where Y_0 is the relative concentration of species Y at time zero and k_2 is a "rate constant" for the photoreaction. (Note that k_2 is equal to $2.303\varepsilon l\phi I_m S/V$. To make comparisons of the "rate constants" possible, the parameters l, I_m, S, and V were kept constant from sample to sample and polymer to polymer.)

$$[Y] = Y_0 e^{-k_2 t} \quad (7)$$

The remaining 99% of the photoreactive starting material that reacts at a slower rate, species X, is in high concentration and is predicted to show the usual zeroth-order kinetics.[54] The resulting rate for the disappearance of X is shown in eq 8, where X_0 is the concentration of species X at time, t, zero and k_1 is the corresponding "rate constant". (k_1 is equal to $\phi I_m S/V$.)

$$[X] = [X_0] - k_1 t \quad (8)$$

By combining eqs 7 and 8, a new overall rate equation for the disappearance of A is formed, eq 9. This equation represents the combined contributions to the overall rate for the two cases derived from the Perrin-like model as illustrated in Figure 4.

$$[A] = X_0 - k_1 t + Y_0 e^{-k_2 t} \quad (9)$$

The Perrin-like expression, eq 9, was used to fit the kinetic traces of polymers **1** and **2**, and the results are illustrated as the solid line in Figure 3a,b. It is apparent that the Perrin-like equation is the best fit for the data at both long and short reaction times. At short reaction times, the dominant species contributing to the observed fast reaction rate is the photogenerated radical species where there is a radical trap in the reaction sphere. The Perrin-like model describes the fast reaction kinetics as a first-order exponential. At longer reaction times, the reaction rate is dominated by the relatively slow reaction that involves migration of a radical trapping species into the reactive sphere of the photogenerated metal radicals. This is described in the Perrin-like model as simple zeroth-order kinetics. The next section will investigate the applicability of the Perrin-like model in other polymer systems by analyzing degradation data found in the literature.

Analysis of a Literature Example Using the Perrin-like Model. To analyze the versatility of the Perrin-like model to other polymer systems, literature data were fit to eq 9. Figure 5 shows data for the photodegradation of polyoxymethylene, **3**, under UV irradiation.[26] (The literature data points were obtained using a literature capture method described in the experimental section of this paper.) The degradation mechanism of polyoxymethylene is known; upon γ irradiation, three radical species are formed: $-O-\dot{C}H-$, $-O-\dot{C}H_2$, and $\dot{O}-CH_2-$.[55,56] The data presented are for the disappearance of the two carbon-centered radicals as monitored by EPR spectroscopy. The kinetic trace for the photodegradation of polymer **3**, like that of polymers **1** and **2**, is biphasic in that there is a fast reaction at short times followed by a slower conversion at extended reaction times.

3

Figure 5a shows the fits of the data for the reaction of polymer **3** to first- and second-order equations (i.e., $C/C_0 = Ae^{-kt}$ and $C/C_0 = (1 + Bt)^{-1}$, respectively). The fits are poor, and therefore these two equations do not accurately represent the reaction mechanism for the degradation of this polymer. Figure 5b shows the fits for the other three models: simple-diffusion, diffusion-controlled, and the Perrin-like model. As was the case with polymers **1** and **2**, it is evident that these three equations more closely fit the data than the first- and second-order equations. Taking a closer look at the initial reaction rates in Figure 5c, it is apparent that both the simple-diffusion and the diffusion-controlled models overestimate the initial reaction rate. This is similar to the findings reported above for polymers **1** and **2**. The Perrin-like model (eq 9), however, fits the data well at both long and short reaction times and is therefore a suitable model for the photodegradation of this polymer system. The interpretation is that the fast, initial rate is due to reaction of the carbon-centered radicals with another photogenerated radical species or an adjacent abstractable atom such as a hydrogen atom in the reaction sphere, and the slower rate is for the reaction of the carbon-centered radicals involving a diffusive reaction.

Fitting Parameters as a Function of Temperature. The photodegradations of polymers **1** and **2** were evaluated as a function of reaction temperature. As in the sections above, the data were fit to first-order, second-order, simple-diffusion, diffusion-controlled, and Perrin-like equations. All data were found to be best fit by the Perrin-like model (eq 9). The parameters obtained from the best fit of the data were plotted as a function of irradiation temperature (Figure 6 and Figure

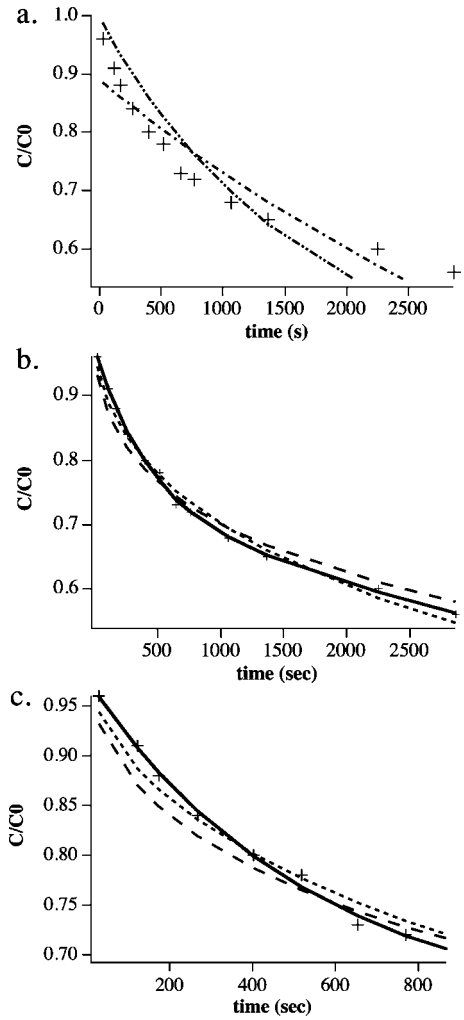

Figure 5. Relative radical concentration as a function of time at 343.5 K following irradiation of polymer **3** (+). The fits are for the first-order (— • —) and second-order (— •• —) equations (a) and simple diffusion (—), diffusion-controlled (**- - -**), and Perrin-like (— — —) fit equations (b). The plot in (c) shows the initial data in plot (b) on expanded axes.

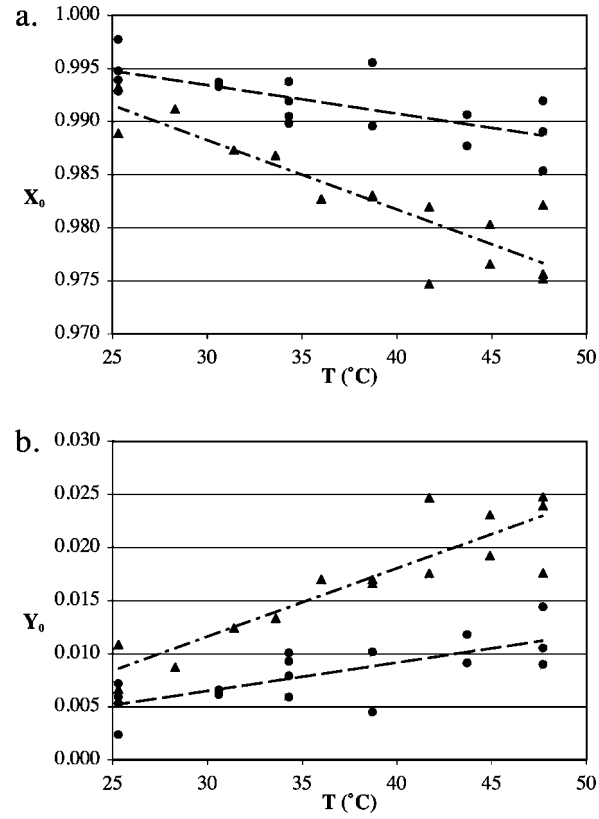

Figure 6. Fitting parameters X_0 and Y_0 from eq 9 as a function of temperature for polymers **1** (▲) and **2** (●).

Table 1. Apparent Enthalpies and Entropies of Activation Obtained from the Eyring Plot of the Rate Constants, k_1 and k_2, versus Temperature for the Photodegradation of Polymers 1 and 2

	k_1 (diffusive)		k_2 (nondiffusive)	
polymer	$\Delta H^{\ddagger}$ (kcal/mol)	$\Delta S^{\ddagger}$ (kcal/(K mol))	$\Delta H^{\ddagger}$ (kcal/mol)	$\Delta S^{\ddagger}$ (kcal/(K mol))
1	7 ± 1	-60 ± 40	2 ± 1	-70 ± 40
2	6 ± 2	-50 ± 40	2 ± 1	-70 ± 40

S1). The parameters Y_0 and X_0 in eq 9 represent the relative concentrations of the photogenerated radical species with and without a radical trapping agent in the reactive sphere, respectively. As shown in Figure 6, Y_0 is small, ranging from 0.5% to 2.5% over the temperature range 25−50 °C. Note also that Y_0 is larger in polymer **1** than in polymer **2**.

The relative ratio of X_0 to Y_0 is dependent on the relative concentration of the radical trapping agent to the concentration of the photogenerated radical. The radical trap (chlorine atom) to metal species (molybdenum) ratio is approximately 100:1 for polymer **1** and 9:1 for polymer **2**. An increase in radical trap concentration with respect to potential metal radical species will increase the probability of a radical trap being located in the reactive sphere. Therefore, it is predicted that polymer **1** would have a larger number of photogenerated radicals with a Cl in the reaction sphere than polymer **2**, i.e., $Y_0(\mathbf{1}) > Y_0(\mathbf{2})$. As shown in Figure 6, this is indeed the case. For example, at room temperature, Y_0 for polymer **1** is ∼0.008 and Y_0 for polymer **2** is 0.005.

For both polymers **1** and **2**, the value of Y_0 increased gradually with an increase in temperature, and there was a corresponding decrease in X_0. (Over the temperature range of the experiment, the value of Y_0 for polymers **1** and **2** increased at a rate of 0.065 ± 0.009% K^{-1} and 0.027 ± 0.007% K^{-1}, respectively.) This trend is likely due to an effective increase in the reaction sphere caused by the enhanced kinetic motion of the radicals and the trapping species. This results in a greater likelihood of a radical trapping agent being in the reactive sphere of the photogenerated radical species.

The experimentally determined values for k_1 and k_2 (eq 9) for polymers **1** and **2** as a function of temperature are shown in Figure S1. Over this temperature range, the value of k_1 (the "rate constant" for the zeroth-order (slower) reaction) ranges from 10^{-6} to 10^{-5} s^{-1}, while k_2 (the "rate constant" for the first-order (faster) reaction) is on the order of 10^{-3} s^{-1}.[57] Restated, the rate constant for the nondiffusive reaction, k_2, is greater than the rate constant for the diffusive reaction, k_1. This result shows that diffusion is the rate-limiting step in the diffusive reaction, as expected.

To extract apparent activation enthalpies and entropies,[58] the data in Figure S1 were fit to an Eyring plot (Figure S2), and the resulting values are shown in Table 1. The enthalpies of activation for the nondiffusive process are much smaller than those for the diffusive process for both polymers **1** and **2**, again consistent with rate-limiting diffusion in the diffusive reaction. The entropies of activation for both processes and polymers are all negative. However, the large relative uncertainties associated with the data preclude firm conclusions at the moment.

Conclusions

The photodegradation rate data of two polymer films, a cross-linked poly(vinyl chloride) and a segmented polyurethane, were compared to six kinetics models. It was found that the degradation did not follow simple zeroth-, first-, or second-order kinetics. Two other models, a simple-diffusion and a diffusion-controlled model, were analyzed and found to more closely represent the data than the zeroth-, first-, and second-order equations. However, these two models still overestimated the initial reaction rates. Accordingly, a new kinetics model, the Perrin-like model, was introduced that utilized basic photochemical rate equations and the heterogeneous nature of solid-state polymers. The equation appropriate to the Perrin-like model fit the data with excellent accuracy. The model was also used to analyze the photodegradation rate of polyoxymethylene, using photodegradation data found in the literature. The Perrin-like model equation was found to be an accurate fit of the literature data presented. An investigation of the effect of temperature on the parameters extracted from the fits to the Perrin-like model showed that only a few percent of the radical species generated had radical trapping agents in the reactive sphere (Perrin-like environment) and that the majority of metal radicals did not have radical trapping agents in the reactive sphere (diffusive environment). It was also found that the apparent $\Delta H^{\ddagger}$ for the photoreaction in the Perrin-like environment was lower than that of the diffusive reaction. It is hypothesized that the rate-limiting step in the diffusive reaction is diffusion together of the photogenerated metal radical and the radical trapping agent.

Acknowledgment. We acknowledge the Petroleum Research Fund, administered by the American Chemical Society, and the National Science Foundation under Grant DGE-0549503 for the support of this research.

Supporting Information Available: Figure showing the change in k_1 and k_2, extracted from the fitting data vs irradiation temperature for polymers **1** and **2**; figure showing the Erying plots for the fitting parameters k_1 and k_2 from eq 9 for polymers **1** and **2**. This material is available free of charge via the Internet at http://pubs.acs.org.

References and Notes

(1) Lamont, W. J. J. *Vegetable Production Using Plasticulture*; Asian and Pacific Region, Food & Fertilizer Technology Center: **1999**.
(2) Maneerat, C.; Hayata, Y. *Trans. ASABE* **2008**, *51*, 163–168.
(3) Guillet, J. E. *Degradable Materials: Perspectives, Issues and Opportunities*; CRC Press: Boca Raton, 1990.
(4) Schnabel, W. *Polymers and Light: Fundamentals and Technical Applications*; Wiley-VCH: Weinheim, 2007.
(5) West, R.; Maxka, J. *ACS Symp. Ser.* **1988**, *360*, 6–20.
(6) West, R. *J. Organomet. Chem.* **1986**, *300*, 327–346.
(7) Ishikawa, M.; Nate, K. *ACS Symp. Ser.* **1988**, *360*, 209–223.
(8) Kijchavengkul, T.; Auras, R.; Rubino, M.; Ngouajio, M.; Fernandez, R. T. *Chemosphere* **2008**, *71*, 1607–1616.
(9) Scott, G. *Trends Polym. Sci.* **1997**, *5*, 361–368.
(10) Lemaire, J.; Arnaud, R.; Dabin, P.; Scott, G.; Al-Malaika, S.; Chohan, S.; Fauve, A.; Maaroufi, A. *Plast. Eng.* **1995**, *29*, 139–149.
(11) Hofer, D.; Miller, R. D.; Willson, C. G. *Proc. SPIE-Int. Soc. Opt. Eng.* **1984**, *469*, 16–23.
(12) Rivaton, A.; Gardette, J.-L.; Mailhot, B.; Morlat-Therlas, S. *Macromol. Symp.* **2005**, *225*, 129–146.
(13) Hwu, J. R.; King, K. Y. *Chem.—Eur. J.* **2005**, *11*, 3805–3815.
(14) Grassie, N.; Scott, G. *Polymer Degradation and Stabilisation*; Cambridge University Press: New York, 1985.
(15) Guillet, J. *Polymer Photophysics and Photochemistry: An Introduction to the Study of Photoprocesses in Macromolecules*; Cambridge University Press: New York, 1985.
(16) Rabek, J. F. *Mechanisms of Photophysical Processes and Photochemical Reactions in Polymers*; Wiley: New York, 1987.
(17) Geuskens, G. *Compr. Chem. Kinet.* **1975**, *14*, 333–424.
(18) Tyler, D. R. *Coord. Chem. Rev.* **2003**, *246*, 291–303.
(19) Tenhaeff, S. C.; Tyler, D. R. *Organometallics* **1991**, *10*, 1116–1123.
(20) Tenhaeff, S. C.; Tyler, D. R. *Organometallics* **1991**, *10*, 473–482.
(21) Tenhaeff, S. C.; Tyler, D. R. *Organometallics* **1992**, *11*, 1466–1473.
(22) Geoffroy, G. L.; Wrighton, M. S. *Organometallic Photochemistry*; Academic Press: New York, 1979.
(23) Meyer, T. J.; Caspar, J. V. *Chem. Rev.* **1985**, *85*, 187–218.
(24) Chen, R.; Tyler, D. R. *Macromolecules* **2004**, *37*, 5430–5436.
(25) Chen, R.; Yoon, M.; Smalley, A.; Johnson, D. C.; Tyler, D. R. *J. Am. Chem. Soc.* **2004**, *126*, 3054–3055.
(26) Shimada, S.; Hori, Y.; Kashiwabara, H. *Polymer* **1981**, *22*, 1377–1384.
(27) Covert, K. J.; Askew, E. F.; Grunkemeier, J.; Koenig, T.; Tyler, D. R. *J. Am. Chem. Soc.* **1992**, *114*, 10446–10448.
(28) Daglen, B. C.; Harris, J. D.; Tyler, D. R. *J. Inorg. Organomet. Polym. Mater.* **2007**, *17*, 267–274.
(29) Daglen, B. C.; Harris, J. D.; Dax, C. D.; Tyler, D. R. *Rev. Sci. Instrum.* **2007**, *78*, 074104/1–074104/4.
(30) Aymard, C.; Shirts, R. B. *J. Chem. Educ.* **2000**, *77*, 1230–1232.
(31) Chen, R.; Meloy, J.; Daglen, B. C.; Tyler, D. R. *Organometallics* **2005**, *24*, 1495–1500.
(32) Bitterwolf, T. E. *Coord. Chem. Rev.* **2001**, *211*, 235–254.
(33) Wrighton, M. S.; Ginley, D. S. *J. Am. Chem. Soc.* **1975**, *97*, 4246–4251.
(34) Krimm, S.; Folt, V. L.; Shipman, J. J.; Berens, A. R. *J. Polym. Sci.* **1963**, *Pt. A1*, 2621–2650.
(35) Tasumi, M.; Shimauouchi, T. *Spectrochim. Acta* **1961**, *17*, 731–754.
(36) De Haseth, J. A.; Andrews, J. E.; McClusky, J. V.; Priester, R. D., Jr.; Harthcock, M. A.; Davis, B. L. *Appl. Spectrosc.* **1993**, *47*, 173–179.
(37) Heintz, A. M.; Duffy, D. J.; Nelson, C. M.; Hua, Y.; Hsu, S. L.; Suen, W.; Paul, C. W. *Macromolecules* **2005**, *38*, 9192–9199.
(38) Elwell, M. J.; Ryan, A. J.; Grunbauer, H. J. M.; Lieshout, H. C. *Polymer* **1996**, *37*, 1353–1361.
(39) Sheth, J. P.; Klinedinst, D. B.; Pechar, T. W.; Wilkes, G. L.; Yilgor, E.; Yilgor, I. *Macromolecules* **2005**, *38*, 10074–10079.
(40) Vandenbelt, J. M.; Henrich, C. *Appl. Spectrosc.* **1953**, *7*, 171–176.
(41) Dogue, L. J.; Mermilliod, N.; Genoud, F. *J. Polym. Sci., Part A: Polym. Chem.* **1994**, *32*, 2193–2198.
(42) Seguchi, T.; Tamura, N. *J. Phys. Chem.* **1973**, *77*, 40–44.
(43) Waite, T. R. *Phys. Rev.* **1957**, *107*, 463–470.
(44) Waite, T. R. *J. Chem. Phys.* **1958**, *28*, 103–106.
(45) Waite, T. R. *J. Chem. Phys.* **1960**, *32*, 21–23.
(46) Shimada, S.; Hori, Y.; Kashiwabara, H. *Polymer* **1977**, *18*, 25–31.
(47) Hori, Y.; Shimada, S.; Kashiwabara, H. *J. Polym. Sci., Polym. Phys. Ed.* **1984**, *22*, 1407–1415.
(48) Bond, G. C. *Metal-Catalysed Reactions of Hydrocarbons*; Springer: Uxbridge, 2005.
(49) McAuley, K. B.; MacGregor, J. F.; Hamielec, A. E. *AIChE J.* **1990**, *36*, 837–850.
(50) Ebewele, R. O. *Polymer Science and Technology*; Chapman & Hall: London, 2000.
(51) Rabek, J. F. *Photodegradation of Polymers Physical Characteristics and Applications*; Springer: New York, 1996.
(52) Perrin, F. *Compt. Rend.* **1924**, *178*, 1978–1980.
(53) Turro, N. J. *Modern Molecular Photochemistry*; Addison-Wesley Publishing Co.: Reading, MA, 1978.
(54) Balzani, V.; Carassiti, V. *Photochemistry of Coordination Compounds*; Academic Press: New York, 1970.
(55) Yoshida, H.; Ranby, B. *J. Polym. Sci., Part A: Gen. Pap.* **1965**, *3*, 2289–2302.
(56) Rabek, J. F. *Polymer Photodegradation: Mechanisms and Experimental Methods*; Chapman & Hall: London, 1995.
(57) Rate constants for zeroth- and first-order reactions have units of M s^{-1} and s^{-1}, respectively. However, because the data were presented and fit as relative concentration versus time, the values of k_1 and k_2 both have units of s^{-1}. For the purpose of comparison, k_1 and k_2 will retain the unit s^{-1} and be referred to as rate constants.
(58) The activation parameters obtained from photochemical reactions as a function of temperature must be interpreted with caution. See ref 54, page 12.

MA8017487